Stereoselective Characterization of the 1,4-Dihydropyridine Binding Site at L-Type Calcium Channels in the Resting State and the Opened/Inactivated State

Klaus-Jürgen Schleifer

Institute for Pharmaceutical Chemistry, Heinrich-Heine-University Düsseldorf, Universitätsstrasse 1, D-40225 Düsseldorf, Germany

Received November 10, 1998

Via a 3D-QSAR pseudoreceptor modeling approach, atomistic binding site models for pharmacologically active 1,4-dihydropyridines (DHPs) were developed. Applying a training set of pure DHP enantiomers a pseudoreceptor model representing the resting state of voltage-gated calcium channels (VGCCs) was generated by correlating experimental versus predicted free energies of binding ($\Delta G°$). For validation further test set derivatives—not used for receptor generation—were predicted yielding root-mean-square (rms) deviation of 0.532 kcal/mol. Selectivity of the resting state model was checked by using the same DHP training set compounds but experimental data for the inactivated channel mode. Although there was found an almost perfect correlation for the training set, the following free relaxation of the corresponding test set applying a Monte Carlo protocol showed rms of 2.033 kcal/mol, clearly demonstrating the lack of any predicting character of the hybrid model. Taking into consideration 19 additional nifedipine analogues, a further verification of the model was performed. This yielded a good correlation for the 12 training set compounds and a satisfactory prediction for the test set molecules with rms of 0.409 kcal/mol. The generation of a pseudoreceptor model depicting the opened/inactivated state of VGCCs required one single additional residue to achieve a rms of 0.848 kcal/mol for the prediction of the test set derivatives. Since all pseudoreceptor models are composed of the same six amino acid residues—Thr, Phe, Gly, Met, Tyr, Tyr—transition from resting to open/inactivated state may be described by one additional hydrogen bond donor interaction (Thr) at the left-hand side of DHPs. Furthermore, a potential charge-transfer interaction for all electron-deficient 4-phenyl DHPs is postulated, because significant correlation between quantum chemically AM1 ($R = 0.91$) and RHF 6-31G** ($R = 0.84$) computed LUMO* energies and experimentally detected $\Delta G°_{exp}$ values was found.

Introduction

Voltage-gated or voltage-operated calcium channels (VGCCs) are transmembrane proteins that mediate the calcium influx in response to membrane depolarization and thereby initiate cellular activities such as secretion, contraction, and gene expression.[1] According to pharmacological and electrophysiological results, they may be divided into the distinct L-, N-, P/Q-, R-, and T-type subfamilies.[2] While all VGCCs are composed of the pore-forming α_1 subunit, the disulfide-linked $\alpha_2\delta$ subunit, and the intracellular β subunit, only the skeletal muscle L-type channel has an additional transmembrane γ subunit.[1] A second special feature of L-type channels is their unique reaction to the therapeutically applied calcium entry blockers such as 1,4-dihydropyridines (DHPs; e.g., nifedipine), phenylalkylamines (e.g., verapamil), and benzothiazepines (e.g., diltiazem) and the exceptional DHP channel activators (BayK 8644, RS30026, CGP 28392, or BayY 5959).[3] However the unique L-type γ subunit is not the physiological target of these compounds, but specific regions of the α_1 subunit.[4,5] Photoaffinity experiments indicated the transmembrane segments S6 in domains III (IIIS6) and IV (IVS6) as the predominant sites of labeling.[6,7] Alanine-scanning mutagenesis[8] and analysis of chimeric calcium channels revealed transmembrane segments IIIS5, IIIS6, and IVS6 as important in DHP binding[9,10] supporting a domain interface model of DHP interaction. Construction of a high-affinity receptor site for DHPs by single amino acid substitutions in a non-L-type calcium channel identified nine residues (IIIS5: Thr1066, Gln1070; IIIS6: Ile1180, Ile1183, Met1188; IVS6: Tyr1490, Met1491, Ile1497, Ile1498; α_{1C-a} numbering) as essential determinants of DHP binding and action and thereby showed conclusively that DHP antagonists and agonists bind to a single receptor site at which they have opposite effects on calcium channel activity.[11−14] Regardless of antagonistic or agonistic effect, receptor affinity of the modulators is dependent on the actual channel mode. While at polarized cell membranes (−70 to −90 mV) channels are in the closed resting state, depolarization starting at −30 mV for L-type VGCCs leads to an oscillation between the opened and inactivated states. Interestingly, all DHP derivatives show higher affinity to their binding site in the opened or inactivated channel mode than to the resting state, but for DHP antagonists this behavior is even more pronounced.[15]

To find a reasonable explanation for this different binding behavior of structurally closely related DHP antagonists and agonists, the aim of the present study was to construct pseudoreceptor models representing

10.1021/jm981114c CCC: $18.00
Published on Web 05/21/1999

minimum requirements of the resting and opened/inactivated states of L-type calcium channels. For this purpose, an atomistic approach was chosen to gain insight into the unknown receptor topology of VGCCs and to clarify potential ligand/binding site interactions on a molecular level.

Methods

DHP Generation. All investigated DHP derivatives were generated within the BUILDER module of the SYBYL software package[16] and energy-minimized applying the conjugate gradients algorithm. To yield consistently geometry-optimized ligand and receptor molecules, the ligands were reoptimized within the PrGen software[17] using the YETI force field.[18] Following semiempirical AM1 single-point energy calculations[19] were performed to yield accurate ESP atomic charges.

Pseudoreceptor Modeling. The pseudoreceptor modeling software PrGen[17] was employed to construct atomistic binding site models for two series of DHP derivatives. This program generates vectors for each functional group of the ligands indicating potential hydrogen bond, lone pair, or hydrophobic interactions. At the tips of these vectors, individually chosen residue templates of an internal database are automatically docked and oriented. Subsequently, a receptor minimization is carried out by energy minimization of all residues keeping position, orientation, and conformation of the training set ligands unaltered. To achieve a high correlation between experimentally derived and calculated binding energies ($\Delta G°_{exp}$ vs $\Delta G°_{calc}$) "correlation coupling" was employed. This additional quantity in the energy term couples the actual rms deviation of $\Delta G°_{calc}$ and $\Delta G°_{exp}$ to the force-field energy of the system. By a straightforward minimization of this term in the course of correlation-coupled receptor minimization, an almost perfect correlation may be enforced. In the next step, the pharmacophore is allowed to relax by minimizing the ligands without constraints while the receptor remains fixed (ligand relaxation). This allows removing strain possibly imposed on the ligands by the receptor during correlation-coupled refinement but usually leads to a less highly correlated model. Therefore, correlation-coupled receptor minimization followed by unconstrained ligand relaxation is repeated until a highly correlated pseudoreceptor model is obtained in the relaxed state (designated as ligand equilibration). To validate the equilibrated receptor, its potency to predict free energies of binding ($\Delta G°_{pred}$) for an external set of ligands (test set) is examined. For this purpose, the test set ligands are minimized within the fixed equilibrated pseudoreceptor applying the same refinement protocol as described for the training set ligands. The linear regression obtained for the training set is used to estimate free energies of binding for the test set derivatives (for more detailed information see Zbinden[20] and Vedani[21]).

In this study, a scaling factor for correlation coupling, so-called coupling constant, of 1.0 and a maximum allowed rms of 0.1 kcal/mol for the calculated versus experimental dissociation constants of all correlation-coupled receptor minimizations were chosen. The target rms deviation was limited to a maximum of 0.130 kcal/mol. Both the training set and test set structures were relaxed without constraints inside the receptor cavity applying 10 trails of a Monte Carlo procedure. Solvation energies of all ligands were calculated according to Still,[22] and entropy corrections were considered following Searle.[23] While biological binding data of the pure DHP enantiomers showing either antagonistic or agonistic activities were taken from Zheng,[24] the experimental data of Bolger[25] and Coburn[26] considering pharmacological effects and dissociation constants of differently substituted 4-phenyl analogues of nifedipine were chosen for the second approach.

Taking into account the Gibbs−Helmholtz equation, conversion of experimental dissociation constants (K_d) to free energies of binding were calculated as follows: $\Delta G°_{exp} = RT \ln(K_d) \cong$ 1.419 (kcal/mol) $\log(K_d)$ at 37 °C and 1.364 (kcal/mol) $\log(K_d)$ at 25 °C, respectively.

HOMO/LUMO Calculations. To evaluate the possibility of charge-transfer interactions between DHP ligands and the pseudoreceptor model, the molecular orbitals of the complexes were calculated employing the semiempirical AM1 method.[19] To yield information about the interrelation between molecular geometry and calculated LUMO energy, isolated DHPs extracted from the pseudoreceptor model and AM1 geometry-optimized derivatives were subjected to AM1 and Hartree−Fock ab initio computations (6-31G** basis set) applying the SPARTAN software package.[27]

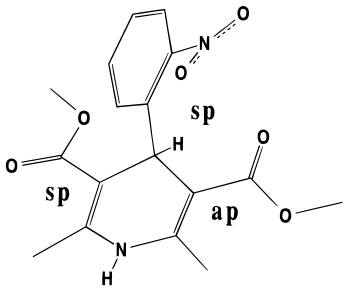

Figure 1. X-ray structure of nifedipine (reference code BICCIZ) with synperiplanar (sp) orientations of the carbonyl oxygen at the left-hand side in relation to the double bond from C2 to C3 and the 2′-nitro group to the hydrogen at C4, respectively. An antiperiplanar (ap) conformation is seen at the right-hand side for the carbonyl oxygen in relation to the double bond from C5 to C6.

Results

Pharmacophore Generation. For the construction of a common pharmacophore for all DHPs, 34 X-ray structures from Cambridge Structural Database[28] and results obtained by earlier ab initio calculations[29] were considered. Taking the X-ray structure of nifedipine as an example, the carbonyl oxygens of the almost coplanar oriented ester side chains may be oriented in a synperiplanar (*Z*)-conformation (sp) or an antiperiplanar (*E*)-conformation (ap) relative to the double bonds of the boatlike DHP ring (Figure 1). Also for the relative spatial orientation of the 2′-nitro group and the hydrogen in position C4, the terms sp and ap are used if both are pointing to the same or opposite side, respectively. To determine the bioactive conformation of DHP ligands with respect to the orientation of their substituents at 3-, 4-, and 5-positions (sp or ap), experimental data of dihydrothieno[2,3-*b*]pyridines (DHTP), sulfur-bridged dihydropyrimidines (SDHPM), and lactone-fused dihydropyrimidines (LDHPM) were taken into account (Figure 2). Focusing on the left-hand side of the molecules, affinity and antagonistic activity are only observed if the carbonyl oxygen resides in sp orientation. Consequently SDHPM are active, while only very weak effects are seen for LDHP with the frozen ap conformation.[30] Also the DHTP derivative S-312, with an sp-like orientation of the isobutyl side chain in 3-position, shows a very high binding affinity (K_i 0.14 nM), whereas the 2-isopropyl derivative is almost inactive (0.26 μM).[31] Comparing the results of the SDHPM, higher affinity (175:1) and stronger effects (722:1) are observed for the 3′-nitro SDHPM in relation to the 5′-nitro derivative[30] indicating a favorable sp conformation at position C4. The situation is more complex on the right-hand side, but information can be derived from investigations of DHTP whereby the *S*- and *R*-enantiomers of S-312 act as potent antagonists (K_i 0.14 and 7.7 nM, respectively).[31] Also for (*S*)-SDHPM and (*R*)-SDHPM pronounced antagonistic and agonistic activity, respec-

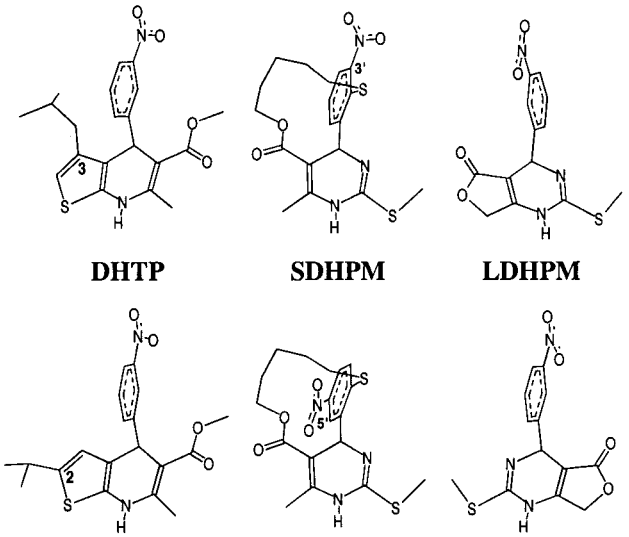

Figure 2. Dihydrothieno[2,3-*b*]pyridines (DHTP) including derivative S-312 (upper left), sulfur-bridged dihydropyrimidines (SDHPM), and lactone-fused dihydropyrimidines (LDHPM) used as semirigid templates for pharmacophore generation.

tively, are observed. In all cases the right-hand side is or may be sp-configured. In contrast to that, neither racemic LDHPM nor its pure enantiomers exert any effects at VGCCs up to concentrations > 30 μM.[30] This clearly demonstrates the importance of an sp orientation of the carbonyl oxygens in C3- and C5-positions as well as the favorable sp orientation of the 4-phenyl substituents.

Pseudoreceptor Model of VGCCs in the Resting State. To generate pseudoreceptor models for DHPs at VGCCs, not all experimentally detected residues crucial for high-affinity binding[11−14] but also other (mainly smaller or more restricted) amino acids with identical functional features were considered. In addition, the minimum number of residues should be taken into account for this approach, because in analogy to other QSAR studies an increasing number of variables decreases the significance of the result. Since both limitations expedited model generation, a multitude of different starting positions and conformations of the template residues could be screened to yield optimum arrangements.

Considering the fact that the only distinction between some of the investigated DHPs is the type of substitution at the left-hand side (C3) or the right-hand side (C5), an analysis of the binding affinities ($\Delta G°_{exp}$) of nitro- and methylcarboxylate-substituted 2′-trifluoromethyl DHPs was carried out (Figure 3). This revealed that disubstituted DHPs (**VIII**, **XII**, and **XIII**) have higher binding affinities compared with the monosubstituted nitro derivatives **VI** and **VII** and that a methyl ester moiety is more favorable ($\Delta G°_{exp}$: **XIII** −8.80 kcal/mol and **XII** −9.70 kcal/mol) than a second nitro group ($\Delta G°_{exp}$: **VIII** −8.26 kcal/mol). On the other hand, the size of the effects is dependent on the side of substitution. If one compares compounds **VI** and **VII**, a nitro group at the right-hand side causes higher free energies of binding compared to the left-hand side ($\Delta G°_{exp}$: **VI** −7.36 kcal/mol vs **VII** −6.97 kcal/mol). The same tendency but more pronounced is seen for disubstituted

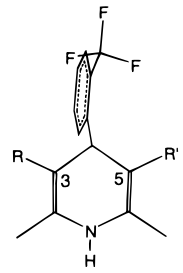

Derivative	R	R'	ΔG^0_{exp}
VI	NO_2	H	-6.97
VII	H	NO_2	-7.36
VIII	NO_2	NO_2	-8.26
XIII	$COOCH_3$	NO_2	-8.80
XII	NO_2	$COOCH_3$	-9.70

Figure 3. Experimentally derived free energies of binding ($\Delta G°_{exp}$) for a series of 2′-trifluoromethyl-substituted DHP derivatives in the resting state of VGCCs (kcal/mol).

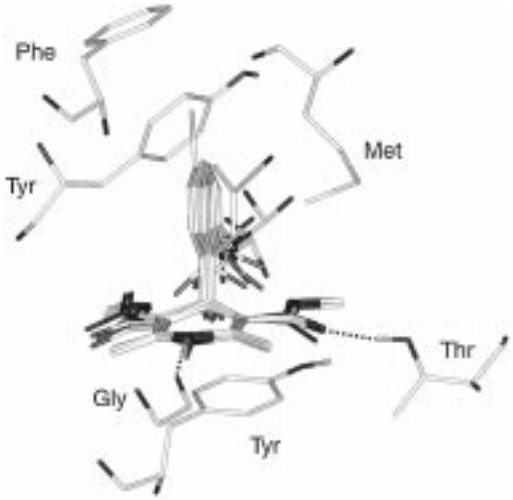

Figure 4. Pseudoreceptor model of L-type VGCCs in the resting state with the used training set derivatives. For clarity only NH and OH hydrogens are displayed (dashed lines indicate hydrogen bonds).

DHPs. In this case a methyl ester at the right-hand side ($\Delta G°_{exp}$: **XII** −9.70 kcal/mol) has more significance for binding than its location at the left-hand side ($\Delta G°_{exp}$: **XIII** −8.80 kcal/mol). This clearly demonstrates the importance of the right-hand side of DHPs for high-affinity binding in the resting state of VGCCs.

In light of these observations, a threonine, which has been experimentally proven to be crucial for binding (Thr1066) was placed as a hydrogen donor at the sp-oriented right side of the pharmacophore. The NH function of the DHP ring was saturated by the carbonyl oxygen of the glycine backbone that imitates the glutamine amide function (Gln1070). A methionine (Met1188 or Met1491) was located axially beside and a phenylalanine on top of the substituted 4-phenyl ring. Two additional tyrosines (Tyr1490) were arranged below the DHP ring and parallel to the 2′- and 3′-substituents, respectively (Figure 4). Correlation-coupled receptor minimization was carried out for all residues of the pseudoreceptor keeping the ligands of the training set fixed. In the following step, correlation-coupled receptor minimization followed by free ligand relaxation was carried out to obtain a satisfactory correlation of R = 0.99 (rms = 0.099 kcal/mol) between experimental and calculated binding energies. To resolve the problem of multiple local minima in conformational space, a Monte Carlo search was performed to find best adjustment of the ligands within the binding cavity. Replacing the training set with the test set ligands followed by an

Table 1. Investigated DHP Antagonists and Agonists with Corresponding Experimentally Determined ($\Delta G°_{exp}$) and Calculated/Predicted ($\Delta G°_{calc}$) Free Energies of Binding (kcal/mol) in the Resting State (rs) of VGCCs[a]

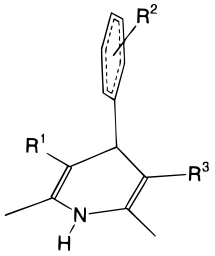

derivative	R^1	R^2	R^3	$\Delta G°_{exp}$ rs	$\Delta G°_{calc}$ rs	ΔG_{solv}
I	$COOCH_3$	2′-NO_2	$COOCH_3$	−10.502	−10.381	−14.198
II	$COOCH_3$	3′-CN	$COOCH_3$	−9.708	−9.784	−10.743
III	$COOCH_3$	4′-Cl	$COOCH_3$	−8.209	−8.176	−9.201
IV	NO_2	2′-OCF_2H	$COOCH_3$	−9.571	−9.660	−14.696
V	$COOCH_3$	2′-OCF_2H	NO_2	−9.264	−9.161	−14.543
VI	NO_2	2′-CF_3	H	−6.967	−6.949	−10.313
VII	H	2′-CF_3	NO_2	−7.364	−7.375	−10.330
VIII	NO_2	2′-CF_3	NO_2	−8.256	−8.453	−17.275
IX	NO_2	2′-OCF_2H	NO_2	−7.817	−7.718	−16.994
X	$COOCH_3$	H	$COOCH_3$	−8.576	−12.083	−8.709
XI	$COOCH_3$	3′-OCH_3	$COOCH_3$	−7.819	−12.767	−9.756
XII	NO_2	2′-CF_3	$COOCH_3$	−9.704	−9.566	−14.150
XIII	$COOCH_3$	2′-CF_3	NO_2	−8.803	−9.294	−13.929
XIV	NO_2	2′-OCF_2H	H	−7.860	−6.965	−10.096
XV	H	2′-OCF_2H	NO_2	−7.422	−7.158	−11.269

[a] Compounds **X**−**XV** represent test set derivatives. Solvation energies of the ligands[22] (ΔG_{solv}) considered for pseudoreceptor generation are indicated in kcal/mol.

unrestricted Monte Carlo relaxation validated the quality of this pseudoreceptor model. Thereafter, free energies of binding were predicted for these test set ligands using the linear regression obtained with the training set yielding a rms of 2.51 kcal/mol (Table 1). As can be seen, the unsatisfactory result for the entire test set showing a deviation of more than 1 K_d unit is mainly caused by the unsubstituted derivative **X** ($\Delta\Delta G°$ −3.51 kcal/mol) and the 3′-methoxy derivative **XI** ($\Delta\Delta G°$ −4.95 kcal/mol). Exclusion of those outliers yields a rms of 0.532 kcal/mol, representing an uncertainty factor (UF) of 2.37 ($=10^{0.532/1.419}$).

Since **X** is the only unsubstituted 4-phenyl derivative and test set molecules usually may only be predicted correctly if related derivatives were used in the training set, the whole procedure was repeated with **X** included in the training set. Surprisingly no sufficient correlation could be found (R = 0.884), indicating again the exceptional character of this compound which will be discussed later.

A further evaluation of this pseudoreceptor model was carried out employing a second set of antagonistically active nifedipine analogues (Table 2). Therefore, the training set ligands within the binding cavity were changed against 12 new ligands of this data set. Correlation-coupled receptor minimization followed by ligand equilibration yielded a correlation of R = 0.998 (rms = 0.121 kcal/mol) for the training set and rms of 2.158 kcal/mol (UF 38.20) for the test set ligands composed of 7 derivatives. Also in this approach, the unsubstituted derivative H* was a member of the test set, and again its free energy of binding was not adequately predicted ($\Delta\Delta G°$ −2.711 kcal/mol). The same energetic overestimation was observed for the 2′- and 3′-methyl derivatives ($\Delta\Delta G°$ −2.992 and −3.954 kcal/mol, respectively). If only the four remaining DHP derivatives (2Br*, 2F*, 3Cl*, and 4Me*) are taken into account, a small deviation from the experimental results is achieved (rms = 0.409 kcal/mol, UF 1.99). Closer

Table 2. Investigated Nifedipine Analogues with Corresponding Experimentally Determined ($\Delta G°_{exp}$) and Calculated/Predicted ($\Delta G°_{calc}$) Free Energies of Binding (kcal/mol) in the Resting State (rs) of VGCCs[a]

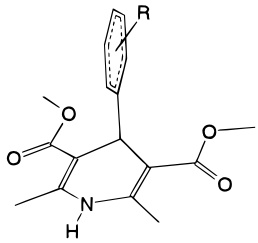

derivative	R	$\Delta G°_{exp}$ rs	$\Delta G°_{calc}$ rs	ΔG_{solv}
2Cl	2′-Cl	−13.340	−13.020	−9.255
2I	2′-I	−14.731	−14.773	−9.178
2NO_2	2′-NO_2	−12.385	−12.386	−14.117
2CN	2′-CN	−12.522	−12.693	−9.742
2OMe	2′-OMe	−10.735	−10.820	−10.468
3CN	3′-CN	−11.840	−11.817	−10.650
3NO_2	3′-NO_2	−13.560	−13.627	−14.651
3F	3′-F	−11.580	−11.704	−9.555
3OMe	3′-OMe	−9.916	−9.895	−9.874
4F	4′-F	−10.175	−10.056	−9.427
4Cl	4′-Cl	−7.666	−7.689	−8.790
F5	2′,3′,4′,5′,6′-F_5	−14.145	−14.115	−9.442
H*		−10.707	−13.418	−8.458
2F*	2′-F	−11.512	−12.107	−9.804
2Br*	2′-Br	−14.308	−13.961	−9.256
2Me*	2′-Me	−11.880	−14.872	−7.993
3Me*	3′-Me	−9.930	−13.884	−8.407
3Cl*	3′-Cl	−12.685	−13.095	−8.938
4Me*	4′-Me	−9.793	−9.955	−8.194

[a] Test set derivatives are indicated with an asterisk (*). Solvation energies of the ligands[22] (ΔG_{solv}) considered for pseudoreceptor generation are indicated in kcal/mol.

inspection of the three outlying ligand/receptor complexes revealed no special interaction to justify such high receptor affinities. Furthermore it is incomprehensible why the only unsubstituted derivative H* should generate more attractive interactions in relation to the substituted derivatives, all the more considering that both tyrosine residues of the receptor surrogate generate strong attractions to the 4-phenyl substituents. Therefore, it is unlikely that PrGen really overestimates the interaction energies of the above-mentioned outliers but, quite the contrary, that the program underestimates the binding energies of all other derivatives. In this case, at least one force being involved in the binding process is not recognized by the implemented YETI force field. Since all molecules of the first approach possess an electron-withdrawing substituent yielding electron-deficient 4-phenyl moieties, one possible explanation of that "unrecognized force" might be a charge-transfer interaction. In this case, an electron transfer should occur from the highest occupied molecular orbital (HOMO) of a receptor residue to the lowest unoccupied molecular orbital (LUMO) of the DHP ligand.

Molecular Orbital Calculations. To prove this hypothesis, three separate complexes, composed of compound **I**/pseudoreceptor (**I**/PR), **II**/pseudoreceptor (**II**/PR), and **X**/pseudoreceptor (**X**/PR), respectively, were extracted from the first pseudoreceptor model and used as input for quantum chemical AM1 calculations. Due to convergence problems in the course of the computations, the models had to be truncated by phenylalanine and one tyrosine residue. Computation of HOMOs and LUMOs indicates striking differences between the complexes. While in all cases HOMOs are localized at the methionine beside the 4-phenyl ring, LUMO of nifedipine (**I**), LUMO+1 of derivative **II**, and only LUMO+5 of compound **X**, respectively, as energetically most favorable unoccupied molecular orbitals at the 4-phenyl moiety (LUMO*s) are detected. Calculation of the orbital energies reveals energy differences between HOMOs and LUMO*s of 7.73, 8.15, and 8.92 eV for **I**/PR, **II**/PR, and **X**/PR, respectively. This demonstrates that electron-deficient 2′-nitro (**I**/PR) and 3′-cyano (**II**/PR) phenyl rings are leading to small energy barriers and therefore favor an electron donor−acceptor interaction.

To probe whether this special property may generally be observed at DHP congeners, the substitution pattern of all investigated nifedipine analogues was examined. This shows a correlation between binding affinity and increasing atomic weight of halogen atoms in 2′-position (Figure 5). Since this correlation is observed only in this particular instance and not independently at any position (compare 4′-position), entropic factors are unlikely to be all-important. On the other hand, halogen-type polarization effects may be assumed as favorable at this location. The 4′-position obviously does not tolerate bulky moieties indicating a lack of space at the complementary locus of the binding site. More complicated is the interpretation of the effects at 3′-position. While methyl and methoxy derivatives possess only weak binding affinities, especially the 3′-nitro DHP is very potent. In general one can observe that electron-withdrawing substituents induce higher $\Delta G°_{exp}$ values related to electron-providing moieties. To characterize the electronic features, all 3′-substituted derivatives as well as compounds H* and F5 were extracted from the second pseudoreceptor model and investigated applying the semiempirical AM1 method. In analogy to the three complexes of the first data set (**I**/PR, **II**/PR, and **X**/PR), HOMOs and LUMO*s were calculated and correlated with the corresponding experimentally derived $\Delta G°_{exp}$ values. In addition, influence of the pseudoreceptor was investigated by successive reduction of the number of considered amino acid residues. Comparison of the results indicates a quite good correlation between the calculated HOMO/LUMO* differences and corresponding experimental binding energies. In all cases not depending on the number of amino acids (4, 3, or 1 residue), a correlation of $R = 0.91$ was found. Surprisingly, also for the LUMO*s of individual DHP derivatives without any pseudoreceptor residue, a correlation of $R = 0.90$ was detected. This allowed quantum chemical ab initio calculations for the isolated DHP congeners with the 6-31G** basis set yielding a slightly worse correlation of $R = 0.86$. Since all quantum mechanical computations are particularly sensitive to conformational distortions and in order to yield a general method to characterize this molecular feature without prior time-consuming pseudoreceptor modeling approach, all derivatives were geometry-optimized using the AM1 method. Calculation of molecular orbitals employing a semiempirical (AM1) and an ab initio method (RHF 6-31G** basis set) reveals significant correlation between LUMO* energies and $\Delta G°_{exp}$ values with coefficients of $R = 0.91$ (AM1; Figure 6) and $R = 0.84$ (6-31G**). Truncation of the investigated data set by the 3′-chloro DHP, which is possibly stabilized via additional polarization interactions (compare 2′-position) yields an even higher correlation of $R = 0.97$ (AM1) and $R = 0.92$ (6-31G**).

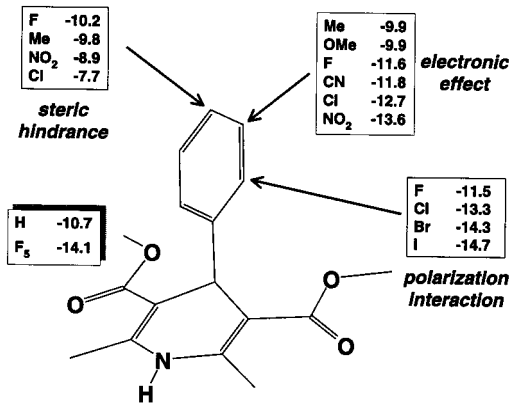

Figure 5. Experimentally derived free energies of binding ($\Delta G°_{exp}$) for a series of ortho-, meta-, and para-substituted nifedipine analogues (kcal/mol). The postulated interaction types for indicated positions are highlighted.

Selectivity of the Pseudoreceptor Model of VGCCs in the Resting State. Since one major objective of this study was the development of selective pseudoreceptor models representing discrete channel modes, the whole model generation was repeated using the first data set (see Table 1) but experimental data of the channel in the opened/inactivated state. Despite a correlation of $R = 0.99$ (rms = 0.115 kcal/mol) for the training set, prediction for the test set molecules with a rms of 5.928 kcal/mol demonstrated the inconsistency

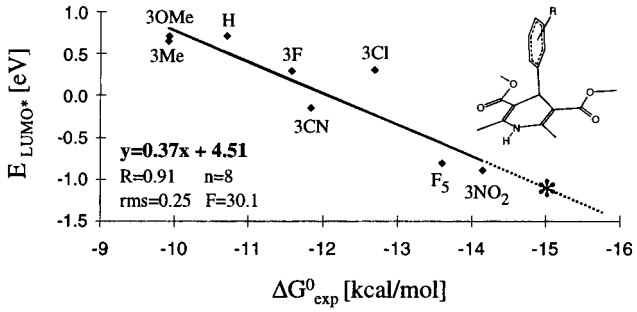

Figure 6. Graph indicating the correlation between semiempirical-derived (AM1) LUMO* energies (eV) and experimental free energies of binding ($\Delta G°_{exp}$) for a series of DHP derivatives. Asterisk on the extrapolated dotted line depicts the calculated LUMO* energy (−1.12 eV) of the most active DHP derivative, isradipine (see Discussion).

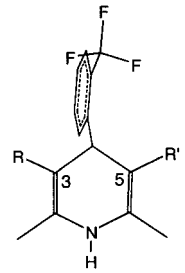

Derivative	R	R'	$\Delta\Delta G^0_{exp}$
VI	NO_2	H	-0.66
VII	H	NO_2	-0.38
VIII	NO_2	NO_2	-0.85
XIII	$COOCH_3$	NO_2	-1.50
XII	NO_2	$COOCH_3$	-0.94

Figure 7. Change of free energies of binding ($\Delta\Delta G°_{exp}$) for a series of 2′-trifluoromethyl-substituted DHPs induced by transition from the resting to the opened/inactivated state of VGCCs (kcal/mol).

of the model. Again, exclusion of derivatives **X** ($\Delta\Delta G°$ −10.79 kcal/mol) and **XI** ($\Delta\Delta G°$ −8.83 kcal/mol) yields a better result with rms = 2.033 kcal/mol. Nevertheless, compared to the findings obtained with experimental data of the channel in the resting state (rms = 0.532 vs 2.033 kcal/mol), the uncertainty factor raises from 2.37 to 27.08, indicating a pronounced differentiation between both channel modes.

Pseudoreceptor Model of VGCCs in the Open/Inactivated State. To gain hints about the varied binding site characteristics of activated channels, changes of the free energies of binding ($\Delta\Delta G°_{exp}$) for some DHP enantiomers were investigated (Figure 7). Comparison of the two monosubstituted nitro derivatives **VI** and **VII** indicates a higher increase in binding affinity if the substituent is located at the left-hand side ($\Delta\Delta G°_{exp}$: −0.66 vs −0.38 kcal/mol). Insertion of a second ($-NO_2$ or $-COOCH_3$) moiety induces stronger DHP binding. Also in this case the methyl ester exerts stronger effects than the nitro group, but significant differences between both substituents may only be observed at the left-hand side ($\Delta\Delta G°_{exp}$: **VIII** −0.85 kcal/mol vs **XIII** −1.50 kcal/mol). Therefore, it may be concluded that mainly substituents at the left-hand side are responsible for pronounced variations, while the right-hand side is only weakly involved in this process.

On the basis of these observations, a second hydrogen donor (e.g., Lys^+, Arg^+, Ser, Gln, and others) was placed at the left side to simulate the opened/inactivated channel mode. After correlation-coupled receptor minimization and ligand equilibration, a threonine yielded best results with a correlation coefficient of $R = 0.99$ (rms = 0.123 kcal/mol) for the training set and rms = 0.848 kcal/mol for the prediction of the residual four test set derivatives (Figure 8). Of course, also for this pseudoreceptor model representing the inactivated state of VGCCs, the expected charge-transfer interactions are observed leading to deviations between experimentally derived and calculated free energies of binding ($\Delta\Delta G°$) of −3.86 and −6.42 kcal/mol for compounds **X** and **XI**, respectively (Table 3).

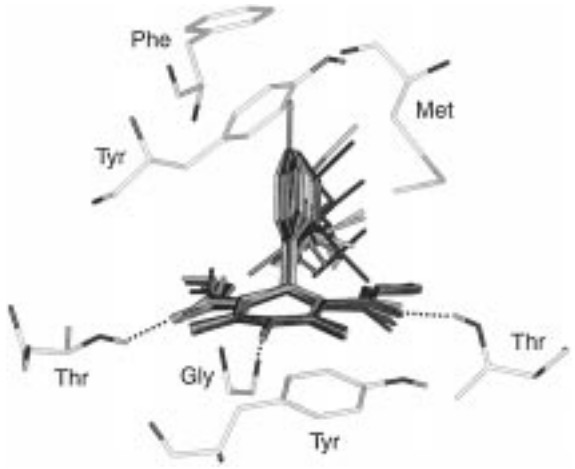

Figure 8. Pseudoreceptor model of L-type VGCCs in the opened/inactivated state showing one additional threonine (Thr) at the left side of DHPs. Only NH and OH hydrogens of all residues, training set (dark gray) and test set (pale gray) derivatives, are displayed. Dashed lines indicate hydrogen bonds.

Table 3. Experimentally ($\Delta G°_{exp}$) and Pseudoreceptor Modeling Approach ($\Delta G°_{calc}$) Derived Free Energies of Binding (kcal/mol) for DHP Antagonists and Agonists in the Opened/Inactivated State (is) of VGCCs[a]

derivative	$\Delta G°_{exp}$ is	$\Delta G°_{calc}$ is
I	−13.184	−13.058
II	−12.108	−12.294
III	−8.964	−9.021
IV	−10.474	−10.499
V	−10.564	−10.430
VI	−7.634	−7.583
VII	−7.741	−7.867
VIII	−9.110	−9.216
IX	−8.660	−8.471
X	−10.387	−14.251
XI	−8.461	−14.877
XII	−10.641	−10.432
XIII	−10.296	−11.284
XIV	−8.277	−7.795
XV	−7.783	−6.509

[a] Compounds **X**−**XV** represent test set derivatives.

Discussion

Mutagenesis experiments revealed the same nine amino acid residues to be crucial for DHP antagonist and agonist binding.[11−14] Therefore, we did not follow the postulated boat and capsized boat model of Rovnyak,[30] which discriminates antagonistically and agonistically active compounds by the up or down orientation of the 4-phenyl ring, but rather a common pharmacophore model for all investigated DHP derivatives that resembles models of Höltje[32] and Goldmann.[33] To find a reasonable explanation for the fact that DHPs show enhanced binding affinities to their binding site in the opened/inactivated state than to the resting state, two different pseudoreceptor models were generated. Use of

amino acids, which as experimentally proven are crucial for binding, makes the models quite realistic. Of course, there is no guarantee that correct placement of residues was achieved, but there are some experimental data to support the chosen positions.

One important interaction of ligands and the pseudoreceptor model is generated via a hydrogen bond between the NH function of DHPs and the carbonyl oxygen of the glycine backbone that mimics the amide group of Gln1070. On the other hand, also alcoholic hydroxyl groups of threonine and tyrosine could serve as hydrogen bond acceptors, but site-directed mutagenesis experiments revealed that an aspartic acid, which is found in VGCCs of carp skeletal muscle, exerts functional similarity to glutamine with respect to DHP interaction.[34] Assuming a direct contact between these crucial residues and the ligands, only the hydrogen-accepting properties of glutamine can be saturated by the carboxylate group of the aspartic acid.

For the postulated hydrogen bond between the accepting nitro or ester groups on the right-hand side of DHPs, the hydroxyl function of threonine was chosen as a donor. At this position also a tyrosine residue with an aromatic hydroxyl group would be conceivable. However, the Tyr1365Phe mutation yields only a loss of 0.7 kcal/mol in free energy of binding for [^{3}H]PN200-110, not supporting the essential function as a hydrogen donor.[35] On the other hand, the electron-providing hydroxyl group of tyrosine increases the electron density of the aromatic ring and makes it a potential candidate to provide the HOMO for the hypothesized charge-transfer interaction. In this situation a Tyr-to-Phe substitution would better fit the experimental findings. Whether or not Met at the right side of the pseudoreceptor models is located accurately cannot be answered, but site-directed mutagenesis experiments and functional assays using two-microelectrode voltage clamp technique demonstrated the essential function of Met1188 for antagonist and agonist effects.[36] In this study, the Val1188Met substitution decreased IC_{50} of isradipine to modulate barium inward currents from $\sim$10 μM to 67 nM (150:1) and enhanced the modulating effect of the agonist BayK 8644 from 1.6 to 3.7 $\pm$ 0.3-fold.

Nevertheless one cannot rule out that (some of) the detected amino acid residues critical for DHP binding have no direct contact to the ligands but merely modulate conformational changes of the channel that regulate access to the binding site.

The postulated transition from resting to opened/inactivated state of VGCCs represented by one additional H-bond interaction at the left side could explain the increased $\Delta G°_{exp}$ values of DHPs in this channel mode. Moreover, the stronger hydrogen bond-accepting potential of carbonyl oxygen (typical for antagonists) in relation to a nitro group (typical for agonists) at that particular location might account for the higher binding affinities of antagonistically active derivatives. However, the accuracy of ligand-based approaches is extremely dependent on structural heterogeneity of the derivatives used for model generation and consistence of the experimental data. Furthermore, the predictive power of such indirect QSAR models is restricted to new molecules with quite similar shapes, volumes, and functional groups with respect to the ligands used for model construction. Therefore, it would be unreasonable to perform predictions for structurally modified DHP ligands whose molecular descriptors are not represented in the training set (e.g., methyl ester- vs isopropyl ester-substituted DHPs) or for quite new chemical structures without any DHP scaffold.

The findings concerning charge-transfer interactions as potential ligand/binding site-stabilizing forces would explain the inappropriate prediction of those derivatives that lack this feature. Due to additional not quantifiable interactions (e.g., polarization effects), the results derived from correlation of LUMO* energies and $\Delta G°_{exp}$ values could not be used to yield satisfactory correlation for all derivatives. Although usually higher sophisticated ab initio calculations provide more reliable results, one explanation for the better correlation achieved in this study with AM1 in comparison to RHF 6-31G** might be the use of experimental data like ionization energies for the development of parameters implemented in semiempirical methods.[19,37] If one takes into account that a correlation of $R = 0.91$ (AM1) was found considering isolated ligands and only one descriptor, this parameter may be a helpful and fast tool for a prescreening of designed ligands. Whether this correlation may be extended onto further substitution patterns must be proven in following investigations. Nonetheless one calculation was carried out to determine the LUMO* of the most active DHP derivative isradipine (PN200-110). Independent of the chosen ester type (isopropyl or methyl ester) a LUMO* energy of -1.12 eV was determined for the 4-benzofurazan (2,1,3-benzoxadiazole) moiety (see Figure 6). This indicates an even higher charge-transfer potential when compared to the most active derivatives F5 (-0.89 eV) and $3NO_2$ (-0.81 eV) investigated in this study.

Conclusion

Although the theoretically derived pseudoreceptor models are unlikely to represent the real binding site, they do allow interpretation of experimental data and reveal new hypotheses about channel activation on a molecular level. More detailed information is expected from refined models based on the recently solved X-ray structure from the homologous voltage-gated potassium channel of *Streptomyces lividans*[38] which we are modeling at present.

Acknowledgment. The author is grateful to Prof. Dr. H.-D. Höltje, Heinrich-Heine-Universität Düsseldorf, for providing all hardware and software facilities and for helpful discussions. Thanks are due to E. Tot for technical assistance and to Dr. S. Goldmann, BAYER AG, Wuppertal, Germany, for some private communication.

References

(1) Jones, S. W. Overview of Voltage-Dependent Calcium Channels. *J. Bioenerg. Biomembr.* **1998**, *30*, 299−312.
(2) Birnbaumer, L.; Campbell, K. P.; Catterall, W. A.; Harpold, M. M.; Hofmann, F.; Horne, W. A.; Mori, Y.; Schwartz, A.; Snutch, T. P.; Tanabe, T.; et al. The Naming of Voltage-Gated Calcium Channels. *Neuron* **1994**, *13*, 505−506.
(3) Striessnig, J.; Grabner, M.; Mitterdorfer, J.; Hering, S.; Sinnegger, M. J.; Glossmann, H. Structural Basis of Drug Binding to L Ca^{2+} Channels. *Trends Pharmacol. Sci.* **1998**, *19*, 108−115.

(4) Regulla, S.; Schneider, T.; Nastainczyk, W.; Meyer, H. E.; Hofmann, F. Identification of the Site of Interaction of the Dihydropyridine Channel Blockers Nitrendipine and Azidopine with the Calcium-Channel α_1 Subunit. *EMBO J.* **1991**, *10*, 45−49.
(5) Nakayama, H.; Taki, M.; Striessnig, J.; Glossmann, H.; Catterall, W. A.; Kanaoka, Y. Identification of 1,4-Dihydropyridine Binding Regions within the α1 Subunit of Skeletal Muscle Ca^{2+} Channels by Photoaffinity Labeling with Diazipine. *Proc. Natl. Acad. Sci. U.S.A.* **1991**, *88*, 9203−9207.
(6) Striessnig, J.; Murphy, B. J.; Catterall, W. A. Dihydropyridine Receptor of L-type Ca^{2+} Channels: Identification of Binding Domains for [^{3}H](+)-PN200−110 and [^{3}H]Azidopine within the α1 Subunit. *Proc. Natl. Acad. Sci. U.S.A.* **1991**, *88*, 10769−10773.
(7) Kalasz, H.; Watanabe, T.; Yabana, H.; Itagaki, K.; Naito, K.; Nakayama, H.; Schwartz, A.; Vaghi, P. L. Identification of 1,4-Dihydropyridine Binding Domains within the Primary Structure of the α1 Subunit of the Skeletal Muscle L-type Calcium Channel. *FEBS Lett.* **1993**, *331*, 177−181.
(8) Peterson, B. Z.; Johnson, B. D.; Hockerman, G. H.; Acheson, M.; Scheuer, T.; Catterall, W. A. Analysis of the Dihydropyridine Receptor Site of L-type Calcium Channels by Alanine-scanning Mutagenesis. *J. Biol. Chem.* **1997**, *272*, 18752−18758.
(9) He, M.; Bodi, I.; Mikala, G.; Schwartz, A. Motif III S5 of L-type Calcium Channels is Involved in the Dihydropyridine Binding Site. A Combined Radioligand Binding and Electrophysiological Study. *J. Biol. Chem.* **1997**, *272*, 2629−2633.
(10) Peterson, B. Z.; Tanada, T. N.; Catterall, W. A. Molecular Determinants of High Affinity Dihydropyridine Binding in L-type Calcium Channels. *J. Biol. Chem.* **1996**, *271*, 5293−5296.
(11) Hockerman, G. H.; Peterson, B. Z.; Sharp, E.; Tanada, T. N.; Scheuer, T.; Catterall, W. A. Construction of a High-Affinity Receptor Site for Dihydropyridine Agonists and Antagonists by Single Amino Acid Substitutions in a non-L-type Ca^{2+} Channel. *Proc. Natl. Acad. Sci. U.S.A.* **1997**, *94*, 14906−14911.
(12) Schuster, A.; Lacinová, L.; Klugbauer, N.; Ito, H.; Birnbaumer, L.; Hofmann, F. The IVS6 Segment of the L-type Calcium Channel is Critical for the Action of Dihydropyridines and Phenylalkylamines. *EMBO J.* **1996**, *15*, 2365−2370.
(13) Grabner, M.; Wang, Z.; Hering, S.; Striessnig, J.; Glossmann, H. Transfer of 1,4-Dihydropyridine Sensitivity from L-type to Class A (BI) Calcium Channels. *Neuron* **1996**, *16*, 207−218.
(14) Mitterdorfer, J.; Wang, Z.; Sinnegger, M. J.; Hering, S.; Striessnig, J.; Grabner, M.; Glossmann, H. Two Amino Acid Residues in the IIIS5 Segment of L-type Calcium Channels Differentially Contribute to 1,4-Dihydropyridine Sensitivity. *J. Biol. Chem.* **1996**, *271*, 30330−30335.
(15) Triggle, D. J.; Rampe, D. 1,4-Dihydropyridine Activators and Antagonists: Structural and Functional Distinctions. *Trends Pharmacol. Sci.* **1989**, *10*, 507−511.
(16) SYBYL, version 6.2; Tripos Associates, Inc., St. Louis, MO.
(17) Zbinden, P. PrGen 1.5.6; Biographics Laboratory: Basel, CH, 1997.
(18) Vedani, A.; Huhta, D. W. A New Force Field for Modeling Metalloproteins. *J. Am. Chem. Soc.* **1990**, *112*, 4759−4767.
(19) Dewar, M. J. S.; Zoebisch, E. G.; Healy, E. F.; Stewart, J. J. P. AM1: A new General Purpose Quantum Mechanical Molecular Model. *J. Am. Chem. Soc.* **1985**, *107*, 3902−3909.
(20) Zbinden, P.; Dobler, M.; Folkers, G.; Vedani, A. PrGen: Pseudo-receptor Modeling Using Receptor-mediated Ligand Alignment and Pharmacophore Equilibration. *Quant. Struct-Act. Relat.* **1998**, *17*, 122−130.
(21) Vedani, A.; Zbinden, P.; Snyder, J. P.; Greenidge, P. A. Pseudo-receptor Modeling: The Construction of Three-Dimensional Receptor Surrogates. *J. Am. Chem. Soc.* **1995**, *117*, 4987−4994.
(22) Still, W. C.; Tempczyk, A.; Hawley, R. C.; Hendrickson, T. Semianalytical Treatment of Solvation for Molecular Mechanics and Dynamics. *J. Am. Chem. Soc.* **1990**, *112*, 6127−6129.
(23) Searle, M. S.; Williams, D. H. The Cost of Conformational Order: Entropy Changes in Molecular Associations. *J. Am. Chem. Soc.* **1992**, *114*, 10690−10697.
(24) Zheng, W.; Stoltefuss, J.; Goldmann, S.; Triggle, D. J. Pharmacologic and Radioligand Binding Studies of 1,4-Dihydropyridines in Rat Cardiac and Vascular Preparations: Stereoselectivity and Voltage Dependence of Antagonist and Activator Interactions. *Mol. Pharmacol.* **1992**, *41*, 535−541.
(25) Bolger, G. T.; Gengo, P.; Klockowski, R.; Luchowski, E.; Siegel, H.; Janis, R. A.; Triggle, A. M.; Triggle, D. J. Characterization of Binding of the Ca^{2+} Channel Antagonist, [^{3}H]Nitrendipine, to Guinea-Pig Ileal Smooth Muscle. *J. Pharmacol. Exp. Ther.* **1983**, *225*, 291−309.
(26) Coburn, R. A.; Wierzba, M.; Suto, M. J.; Solo, A. J.; Triggle, A. M.; Triggle, D. J. 1,4-Dihydropyridine Antagonist Activities at the Calcium Channel: A Quantitative Structure−Activity Relationship Approach. *J. Med. Chem.* **1988**, *31*, 2103−2107.
(27) SPARTAN 3.0; Wavefunction, Inc., Irvine, CA.
(28) Cambridge Structural Database, Cambridge Crystallographic Data Centre, 12 Union Rd, Cambridge CB2 1EZ, U.K.
(29) Schleifer, K.-J. Quantum Chemical Generation of a Nifedipine Pharmacophore Model. *Pharm. Pharmacol. Lett.* **1995**, *5*, 162−165.
(30) Rovnyak, G. C.; Kimball, S. D.; Beyer, B.; Cucinotta, G.; DiMarco, J. D.; Gougoutas, J.; Hedberg, A.; Malley, M.; McCarthy, J. P.; Zhang, R.; Moreland, S. Calcium Entry Blockers and Activators: Conformational and Structural Determinants of Dihydropyrimidine Calcium Channel Modulators. *J. Med. Chem.* **1995**, *38*, 119−129.
(31) Adachi, I.; Yamamori, T.; Hiramatsu, Y.; Sakai, K.; Mihara, S.-I.; Kawakami, M.; Masui, M.; Uno, O.; Ueda, M. Studies on Dihydropyridines. III. Synthesis of 4,7-Dihydrothieno[2,3-*b*]-pyridines with Vasodilator and Antihypertensive Activities. *Chem. Pharm. Bull.* **1988**, *36*, 4389−4402.
(32) Höltje, H.-D.; Marrer, S. A Molecular Graphics Study on Structure-Action Relationships of Calcium-Antagonistic and Agonistic 1,4-Dihydropyridines. *J. Comput.-Aided Mol. Des.* **1987**, *1*, 23−30.
(33) Goldmann, S.; Stoltefuss, J. 1,4-Dihydropyridine: Einfluss von Chiralität und Konformation auf die Calcium-antagonistische und -agonistische Wirkung. (1,4-Dihydropyridines: Influence of Chirality and Conformation to the Calcium Antagonistic and Agonistic Effect.) *Angew. Chem.* **1991**, *103*, 1587−1605.
(34) Mitterdorfer, J.; Wang, Z.; Sinnegger, M. J.; Hering, S.; Striessnig, J.; Grabner, M.; Glossmann, H. Two Amino Acid Residues in the IIIS5 Segment of L-type Calcium Channels Differentially Contribute to 1,4-Dihydropyridine Sensitivity. *J. Biol. Chem.* **1996**, *271*, 30330−30335.
(35) Peterson, B. Z.; Tanada, T. N.; Catterall, W. A. Molecular Determinants of High Affinity Dihydropyridine Binding in L-type Calcium Channels. *J. Biol. Chem.* **1996**, *271*, 5293−5296.
(36) Sinnegger, M. J.; Wang, Z.; Grabner, M.; Hering, S.; Striessnig, J.; Glossmann, H.; Mitterdorfer, J. Nine L-type Amino Acid Residues Confer Full 1,4-Dihydropyridine Sensitivity to the Neuronal Calcium Channel α_{1A} Subunit. Role of L-type Met1188. *J. Biol. Chem.* **1997**, *272*, 27686−27693.
(37) Dewar, M. J. S.; Thiel, W. Ground States of Molecules. 39. MNDO Results for Molecules Containing Hydrogen, Carbon, Nitrogen, and Oxygen. *J. Am. Chem. Soc.* **1977**, *99*, 4907−4917.
(38) Doyle, D. A.; Cabral, J. M.; Pfuetzner, R. A.; Kuo, A.; Gulbis, J. M.; Cohen, S. L.; Chait, B. T.; MacKinnon, R. The Structure of the Potassium Channel: Molecular Basis of K^+ Conduction and Selectivity. *Science* **1998**, *280*, 69−77.

JM981114C